Biosensors and Bioelectronics xx (xxxx) xxxx–xxxx

Contents lists available at ScienceDirect

Biosensors and Bioelectronics

journal homepage: www.elsevier.com/locate/bios

Zwitterionic peptide anchored to conducting polymer PEDOT for the development of antifouling and ultrasensitive electrochemical DNA sensor

Guixiang Wang[a,b], Rui Han[a], Xiaoli Su[a], Yinan Li[a], Guiyun Xu[a], Xiliang Luo[a,*]

[a] Key Laboratory of Sensor Analysis of Tumor Marker, Ministry of Education, College of Chemistry and Molecular Engineering, Qingdao University of Science and Technology, Qingdao 266042, China

[b] College of Chemistry and Chemical Engineering, Taishan University, Taian 271021, PR China

ARTICLE INFO

Keywords:
Antifouling biosensor
Peptide
Electrochemistry
PEDOT
Cancer biomarker
DNA

ABSTRACT

Zwitterionic peptides were anchored to a conducting polymer of citrate doped poly(3,4-ethylenedioxythiophene) (PEDOT) via the nickel cation coordination, and the obtained peptide modified PEDOT, with excellent antifouling ability and good conductivity, was further used for the immobilization of a DNA probe to construct an electrochemical biosensor for the breast cancer marker BRCA1. The DNA biosensor was highly sensitive (with detection limit of 0.03 fM) and selective, and it was able to detect BRCA1 in 5% (v/v) human plasma with satisfying accuracy and low fouling. The marriage of antifouling and biocompatible peptides with conducting polymers opened a new avenue to construct electrochemical biosensors capable of assaying targets in complex biological media with high sensitivity and without biofouling.

1. Introduction

Developing stable, sensitive, and selective biosensors to achieve the early detection of cancer biomarkers is of great significance (Wang et al., 2015a; Wu et al., 2015). In the past years, a great deal of effort has been devoted to the exploration of new technologies to detect early signs of diseases (Luo and Davis, 2013; Wu and Qu, 2015). However, nonspecific protein adsorption on sensing interfaces seriously affects the efficacy of biosensors. Therefore, functional materials that can prevent nonspecific protein adsorption from actual complex media and meet the needs of practical applications have received increasing attention. Poly(ethylene glycol) (PEG) and oligo(ethylene glycol) (OEG) have been the most widely used antifouling materials owing to their surface hydration (Ladd et al., 2009; Lowe et al., 2015; Luo et al., 2014; Vaisocherová et al., 2015). However, PEG and OEG are susceptible under oxidative condition that has limited their utility for long-term applications. Another major type of antifouling materials are zwitterionic polymers, such as poly(sulfobetainemethacrylate) (Chang et al., 2013) and poly(carboxybetainemethacrylate) (Luo et al., 2013; Sundaram et al., 2014), and they have strong hydration through ionic solvation. It has been reported that zwitterionic poly[2-(methacryloyloxy) ethyl phosphorylcholine] brushes exhibited much stronger protein resistance ability than PEG coatings (Yoshimoto et al., 2009). But so far, zwitterionic reagents that can be introduced onto substrate surfaces to render them antifouling ability are usually limited to betaine and phosphorylcholine related chemicals (Xu et al., 2015), whose synthetic processes are time-consuming and complicated.

Peptides, which are composed of natural amino acids, exist predominantly as zwitterions at isoelectric point in aqueous solutions because of the formation of deprotonated carboxyl groups and protonated amine groups. Currently, peptides are usually synthesized by a solid-phase technique (Nowinski et al., 2012; Chen et al., 2009), and the synthetic process is considerably quick and convenient. Moreover, peptides are normally of biocompatible nature, which make them suitable for the synthesis of zwitterionic biomaterials. For example, Jiang's group has synthesized a peptide (EKEKEKE) that exhibited strong antifouling feature to lysozyme and fibrinogen, respectively (Chen et al., 2009; Nowinski et al., 2012). Ye et al. have also reported a zwitterionic peptide with the sequence of CRERERE that showed good resistance to single protein adsorption (Ye et al., 2015). Although these peptides exhibited excellent antifouling performances, their applications in the construction of biosensors and assaying in complex media have rarely been reported.

To build antifouling surfaces with peptides, it is important to immobilize them onto interfaces with well-ordered structure and high surface density. A synthetic thiol anchor (such as $[NH_2(CH_2)_4–SH]$ or 3-mercaptopropionic acid) was currently the most popularly used strategy for attaching functionalized peptides to gold substrates (Bolduc et al., 2010; Chen et al., 2009). The amino acid cysteine (C), which contains an active thiol side group, has also been frequently used

* Corresponding author.
E-mail address: xiliangluo@qust.edu.cn (X. Luo).

http://dx.doi.org/10.1016/j.bios.2016.10.088
Received 26 August 2016; Received in revised form 1 October 2016; Accepted 27 October 2016
Available online xxxx
0956-5663/

to attach peptides onto gold surfaces (Ye et al., 2015). However, it is difficult to obtain peptide layers/films with high surface density and well-ordered structure through this method, and in addition, this method is only applicable to gold substrates. Therefore, it is still highly desirable to develop simple and convenient anchoring strategies to achieve peptide based antifouling surfaces.

Herein, in light of the report of Rao and coworkers, where nickel cations were found to be able to bridge carboxyl groups between different chemicals through the formation of nickel complexes (Yao et al., 2007), we constructed a novel low fouling electrochemical biosensor based on peptides (sequence EKEKEKE) anchored to a conducting polymer, poly(3,4-ethylenedioxythiophene) (PEDOT) doped with citrate ions, which are rich in carboxyl groups. In this work, BRCA1, a gene closely related to breast cancer (Skolnick, 1994; Kuhl et al., 2000), was selected as the target. Firstly, a layer of conducting polymer PEDOT possessing suitable conductivity, biocompatibility and stability (Cui et al., 2016) was directly electrodeposited on glassy carbon electrode (GCE) in a solution containing 3,4-ethylenedioxythiophene (EDOT) and sodium citrate. During the process of deposition, citrate ions with three negatively charged carboxyl groups were incorporated in the formed PEDOT conducting polymer as dopant, and some of the carboxyl groups on the surface were used for the following immobilization of peptide, as shown in Scheme 1. Briefly, nickel cations were introduced to bridge carboxyl groups from the PEDOT film surface and peptides through the formation of Ni–O coordination bonds. Peptides anchored on the PEDOT film were further used for the immobilization of the BRCA1 recognition probe (terminated with carboxyl group) through the formation of amide bonds, and thus the DNA sensor was successfully fabricated.

2. Materials and methods

2.1. Regents

Sodium citrate, 3,4-ethylenedioxythiophene (EDOT), $NiCl_2{\cdot}6H_2O$, bovine serum albumin (BSA) and human serum albumin (HSA) were purchased from Aladdin Reagents (Shanghai, China). $Co(phen)_3(ClO_4)_3{\cdot}3H_2O$ were synthesized according to literature. (Dollimore and Gillard, 1973) Peptides (sequence is EKEKEKE, a purity of > 95%) (Chen et al., 2009) and BREA1 (Ludwig et al., 1997) breast cancer gene were both ordered from Sangon Biotench Co., Ltd (Shanghai, China) and purified by high-performance liquid chromatography (HPLC) and used as received. DNA sequences were as follows (Wang et al., 2015b):

capture DNA (ssDNA): 5′-COOH-GAT TTT CTT CCT TTT GTT C-3′;

target DNA: 5′-GAA CAA AAG GAA GAA AAT C-3′;

one-base mismatch (M_1): 5′-CAA CAA AAG GAA GAA AAT C-3′;

three-base mismatch (M_2): 5′-CAA CAA AAG CAA CAA AAT C-3′;

complete mismatch (M_3): 5′-CCT TGT TGG ACT CCC TTC-3′.

Stock solutions of DNA were prepared with phosphate buffered saline (PBS, 10 mM, pH 7.4) and stored in a freezer at 4 °C before use. N-hydroxysuccinimde (NHS) and 1-ethyl-3-(3-dimethyl- aminopropyl) carbodiimide (EDC) were purchased from Sigma Aldrich. Human plasma samples were provided by the Hospital of Taishan University. Other reagents were of analytical grade. Millipore water obtained from a Milli-Q water purifying system was used throughout.

2.2. Apparatus

Electrochemical experiments were performed on a CHI 650E electrochemical workstation (Shanghai Chenhua Instrument Co. Ltd., China). A conventional three-electrode system was used with a glassy carbon working electrode (GCE, 3.0 mm in diameter), a platinum wire counter electrode and a saturated calomel reference electrode (SCE). The pH values of all solutions were measured with Sartorius PB-10 pH meter (Beijing, China).

The water contact angle measurement was performed on the JC2000-CG400 goniometer of Zhongchen Digital Technical Co. (Shanghai, China) at ambient humidity and temperature by the sessile drop method. The top surface and cross-section morphologies of the PEDOT were characterized using field emission scanning electron microscope (SEM) (JEOL JSM-7500F, Hitachi High-Technology Co., Ltd., Japan). X-ray photoelectron spectroscopy (XPS) measurements were performed using an ESCALAB 250Xi spectrometer (Thermo Fisher Scientific, UK) with a monochromatic Al Kα X-ray source. All spectra were calibrated by normalizing the C (1s) peak to the standard value of 285.0 eV.

2.3. Electrodeposition of PEDOT on GCE surface

GCE was polished with alumina slurries with the diameter of 1.0, 0.3 and 0.05 μm in sequence, and then was cleaned by Millipore water, 100% ethanol and Millipore water for 2 min, respectively. Negatively charged carboxyl groups of sodium citrate can be used as dopant for the electrochemical polymerization of PEDOT. 5 mL water containing 0.02 M EDOT and 0.0434 g sodium citrate were ultrasonic treatment 20 min and then electrodeposited on GCE surface with a constant potential of 1.1 V for 200 s, followed by rinsing with water and drying in a nitrogen stream.

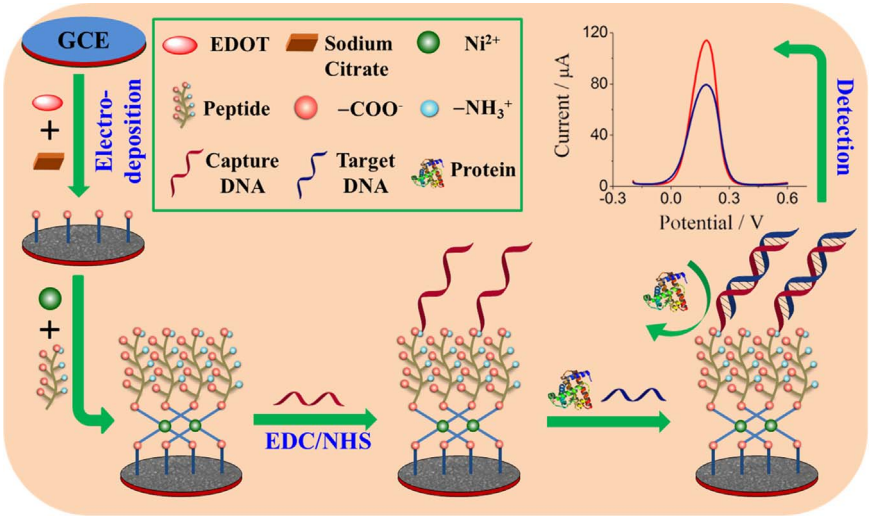

Scheme 1. Schematic illustration of the fabrication process of the DNA sensor.

2.4. Fabrication of the DNA sensor

The fabrication process of the gene biosensor using the prepared film of PEDOT- Citrate is shown in Scheme 1. The GCE/PEDOT-Citrate was immersed into $NiCl_2$ containing (1 mM) borate buffer solution (10 mM, pH 7.5) incubating at 45 °C for 20 min, and then dipped into water to rinse gently. GCE/PEDOT-Citrate/Ni^{2+} was obtained and then immediately immersed into peptide solution (50 μM, prepared with 10 mM borate buffer solution , pH 6.5) and incubated at 45 °C for 30 min. GCE/PEDOT-Citrate/Ni^{2+}/Peptide was also obtained after rinsed and soaked in phosphate buffered saline (PBS, 10 mM, pH 7.4) for one day to equilibrate the peptide (Luo et al., 2013). 1 μM ssDNA was incubated in a solution containing 0.4 M EDC and 0.1 M NHS for 30 min, and then the above solution (20 μL) were drop-coated to the electrode surface for 2 h at ambient temperature keeping the electrode surface wet. After extensively washing with PBS (10 mM, pH 7.4), a fairly stable biosensor (GCE/PEDOT-Citrate/Ni^{2+}/Peptide/ssDNA) was obtained, and it was stored at the refrigerator at 4 °C before use. After the determination of samples, the modified electrode was rinsed with PBS and then stored or used for the following determination of targets with higher concentrations (similar to other affinity biosensors, the used biosensor can detect samples with increasing target concentrations, and in order to detect sample with lower target concentration, the biosensor need to be regenerated to disassociate the bound targets).

2.5. Electrochemical measurements

Differential pulse voltammetry (DPV) is a sensitive and powerful technique of quantitative detection. DPV measurements were carried out in PBS (10 mM, pH 7.4) containing 5.0 mM $[Fe(CN)_6]^{3-/4-}$ and 0.1 M KCl. The scan range was taken from −0.2 V to 0.6 V with incr. E 0.004 V, amplitude 0.05 V, pulse width 0.05 s, sampling width 0.0167 V and pulse period 0.2 s. After hybridization with different concentration of the target DNA, the current changes were recorded accordingly.

Electrochemical impedance spectroscopy (EIS) measurements were recorded in 1.0 mM $[Fe(CN)_6]^{3-/4-}$ or $Co(phen)_3^{3+/2+}$ solution containing 0.1 M KCl within a frequency range of 0.01–100,000 Hz. The direct current potential was set at 0.20 V. The amplitude of the applied sine wave was 5 mV and the impedance spectras were plotted in the form of Nyquist plots.

3. Results and discussions

3.1. Characterization of the PEDOT film

The morphology of the PEDOT film electrodeposited on the electrode surface was characterized by SEM. As shown in Fig. 1A, the surface of the PEDOT film was relatively uniform, and it was composed of particles with a diameter of about 50 nm. According to the image of the cross-section of the PEDOT film, it was clear that PEDOT was evenly covered on the electrode surface, and the thickness of the PEDOT film was about 210 nm (Fig. 1B).

As the conducting polymer PEDOT was doped with citrate ions that contain carboxyl groups, it is expected that there will be free carboxyl groups on the surface of PEDOT that may be used for further functionalization. To confirm that the PEDOT surface contains carboxyl group, EIS and contact angle measurements were employed. As shown in Fig. S1, the electrodeposited PEDOT film on the GCE showed a much higher charge-transfer resistance (R_{ct}) for negatively charged $[Fe(CN)_6]^{3-/4-}$ probes than that for positively charged $[Co(phen)_3]^{3+/2+}$ probes. This result was in accordance with the fact that PEDOT film possesses many negatively charged carboxyl groups which have strong electrostatic repulsion to negatively charged $Fe(CN)_6^{3-/4-}$ while electrostatic attraction to positively charged $Co(phen)_3^{3+/2+}$ probes.

As can be seen from Fig. S2, the water contact angle of the PEDOT film showed a clear transition from 73 ± 3° to 40.5 ± 3° when the pH of the measuring solution was changed from 2.03 to 11.05, indicating that many carboxyl groups were presented on the PEDOT surface and they changed from –COOH to $–COO^-$ (deprotonated at basic solution), and the formation of more negatively charged $–COO^-$ at higher pH value made the surface more hydrophilic (Li et al., 2007; Weng et al., 2016). Therefore, the surface of PEDOT film possessed sufficient carboxyl groups to coordinate nickel ions for the immobilization of peptides and further construction of biosensors.

3.2. Characterization of the DNA sensor fabrication process

The fabrication process of the biosensor was monitored using DPV. As can be seen from Fig. 2, the oxidation peak current of the $[Fe(CN)_6]^{3-/4-}$ probe on the PEDOT modified electrode (curve b) was significantly lower than that on the bare GCE (curve a). This current decrease may be ascribed to two main reasons: the poor conductivity of the conducting polymer (though still conductive), and the charge repulsion of the conducting polymer with carboxyl groups (negatively charged) to the negatively charged $[Fe(CN)_6]^{3-/4-}$ probes. After peptides were immobilized onto the surface of PEDOT film with the aid of nickel cation coordination, the peak current of the redox probe at the modified electrode increased drastically (curve c), and the reason for this change was mainly owing to the positive charge and good conductivity of nickel cations that can promote the charge transfer of the probe. Following the immobilization of the capture DNA (BRCA1 recognition probe, denoted as ssDNA), the peak current decreased slightly (curve d), indicating that ssDNA was successfully immobilized

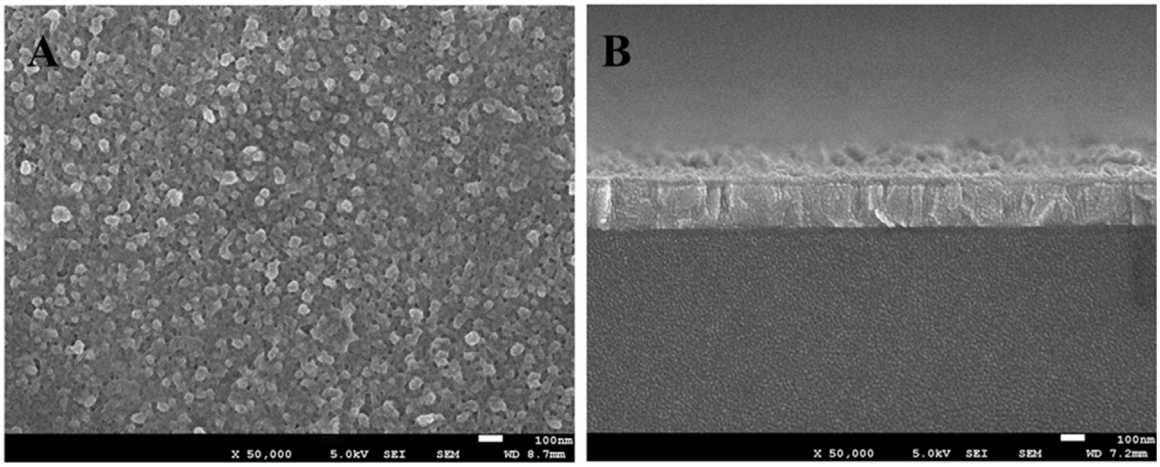

Fig. 1. SEM images of PEDOT film (A: top view; B: side view).

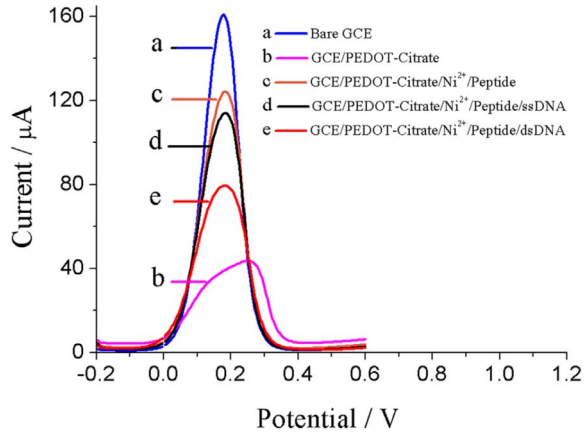

Fig. 2. DPV curves of different electrodes recorded in PBS (10 mM, pH 7.4) containing 5.0 mM $[Fe(CN)_6]^{3-/4-}$ and 0.1 M KCl.

and its negatively charged phosphate skeletons can repel the negatively charged probes to reach the electrode surface. Interestingly, a significant decrease in peak current was observed after hybridization with the target DNA, which can be ascribed to the enhanced electrostatic repulsion of the negatively charged probe associated with the binding of target DNA with negatively charged phosphate skeletons. Clearly, this peak current change along with the selective binding of target DNA can be adopted as sensing signal of the DNA sensor.

Fig. 3 shows the XPS survey scans of electrode surfaces after PEDOT-Citrate film deposition, Ni^{2+}-Peptide attachment, and ssDNA immobilization, respectively. Carbon (C), oxygen (O) and sulfur (S) were characteristic elements of the PEDOT (C and O are also characteristic elements of the citrate), and their photoelectron peaks appeared at 285 eV (C_{2S}), 533 eV (O_{2S}), 163 eV (S_{2p}) and 227 eV (S_{2S}), respectively, indicating that PEDOT-Citrate composites were successfully electrodeposited (Fig. 3A) (Stockhausen et al., 2015). After the treatment with Ni^{2+} and peptide, three new peaks appeared: Nitrogen (N_{1S}), the characteristic element coming from the peptide, appears at 399 eV; the other two peaks corresponding to Ni^{2+} and Cl^-, appear at 855 eV and 197 eV, respectively. Finally, after the immobilization of the capture DNA, a new weak peak appeared at 135 eV (Fig. 3C, inset), which was the characteristic element of phosphorus (P) for ssDNA. Besides, the relative intensity of nitrogen peak in Fig. 3C is stronger than that in Fig. 3B, because of the contribution of P from DNA's four bases (Imani et al., 2015). Therefore, it was clear that PEDOT, peptide and DNA probe were successfully modified onto the electrode surface in sequence.

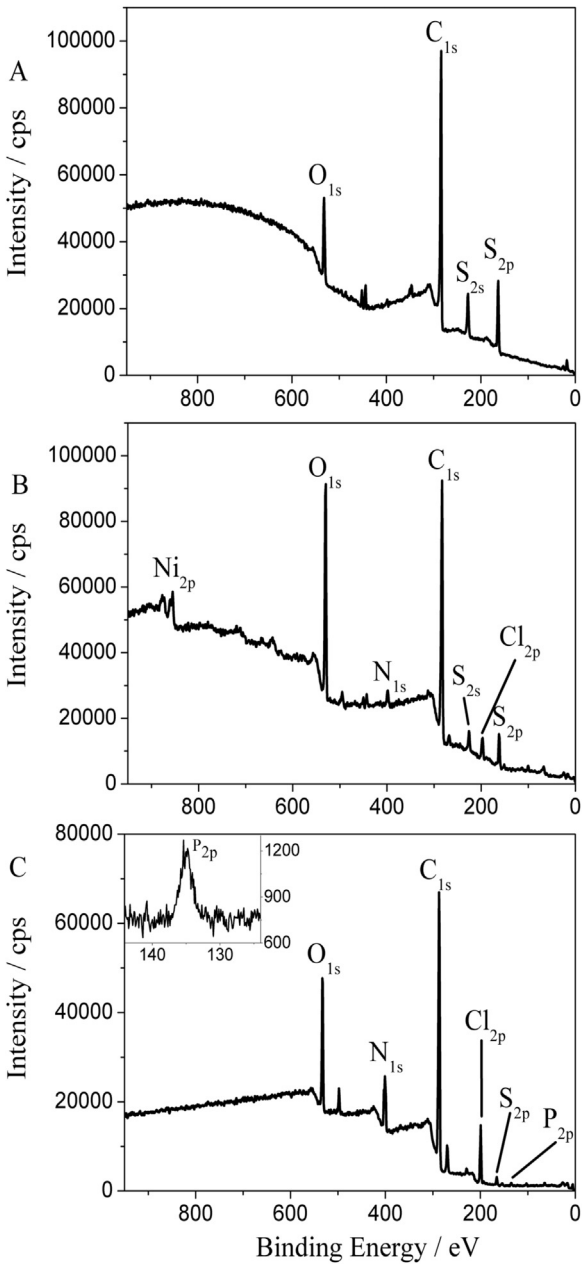

Fig. 3. XPS spectra of electrode surfaces modified with (A) PEDOT-Citrate, (B) PEDOT-Citrate /Ni^{2+}/Peptide, and (C) PEDOT-Citrate/Ni^{2+}/Peptide/ssDNA.

3.3. Optimization of experimental conditions

To maximize the sensitivity and efficiency of the gene biosensor, the optimization for the Ni^{2+} coordination temperature, Ni^{2+} coordination time, the pH of Ni^{2+} solution, the pH of peptide solution, the peptide concentration and peptide coordination time were investigated.

As shown in Fig. S3 A–F, after detailed investigation, the optimized conditions were as follow: (A) Nickel ion coordination temperature, 45 °C; (B) Nickel ion coordination time, 20 min; (C) Nickel ion coordination pH, pH 7.5; (D) Peptide solution pH, pH 6.5; (E) Peptide concentration, 50 μm; and (F) Peptide coordination time, 30 min

3.4. Sensing performance of the DNA sensor

To assess the analytical performance of the prepared biosensor, under optimal conditions, a series of target DNA concentrations were detected by DPV (Fig. 4). Clearly, the DPV peak current decreased along with the increase of the target DNA concentration (Fig. 4A). A good linear relationship between the biosensor response and the logarithm of the target DNA concentration was obtained ranging from 1.0×10^{-16} M to 1.0×10^{-10} M (Fig. 4B). The linear regression equation was ΔI (μA)=3.131 Log$C$ (M) +61.67, with a correlation coefficient of 0.9960, and the detection limit was calculated to be as low as 0.03 fM (S/N=3), which is much lower than previous report (about 1.72 fM) (Wang et al., 2015b).

3.5. Antifouling, selectivity and reproducibility property of the DNA sensor

In order to evaluate the antifouling property of the biosensor, its response changes after soaking in human serum albumin (HSA) solution and human plasma (to excluded possible response change related to target binding, biosensors were saturated with target DNA before soaking in plasma samples) were recorded, respectively (Fig. 5). Clearly, compared with electrode modified with only PEDOT film, the

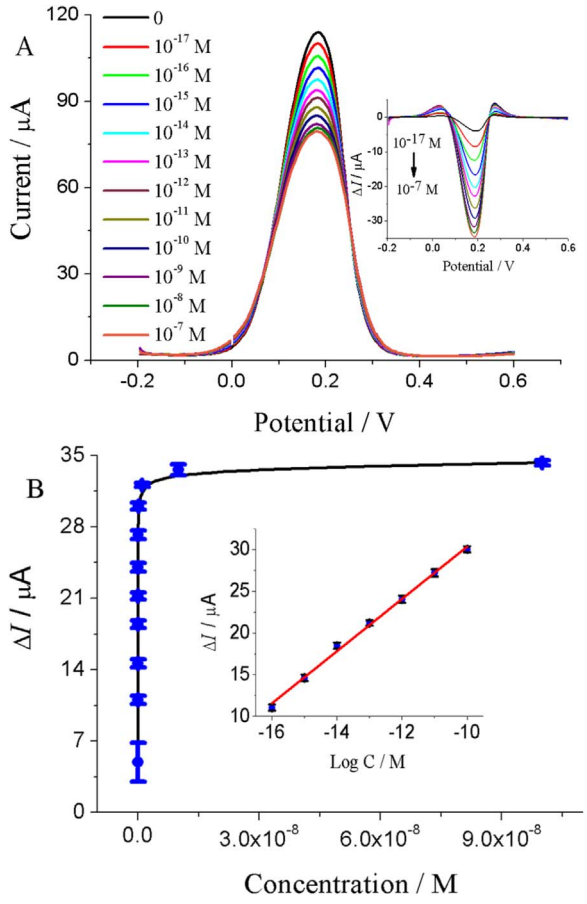

Fig. 4. (A). DPV curves of the biosensor after incubation in different target DNA concentrations (PBS, 10 mM, pH 7.4). Inset: DPV curves after background subtraction. (B). Corresponding response curve of the biosensor. Inset: calibration curve of gene biosensor. Error bars represent the standard deviations of three repeated measurements, and the relative standard deviations (RSDs) at different concentrations are within 1.18–3.42%.

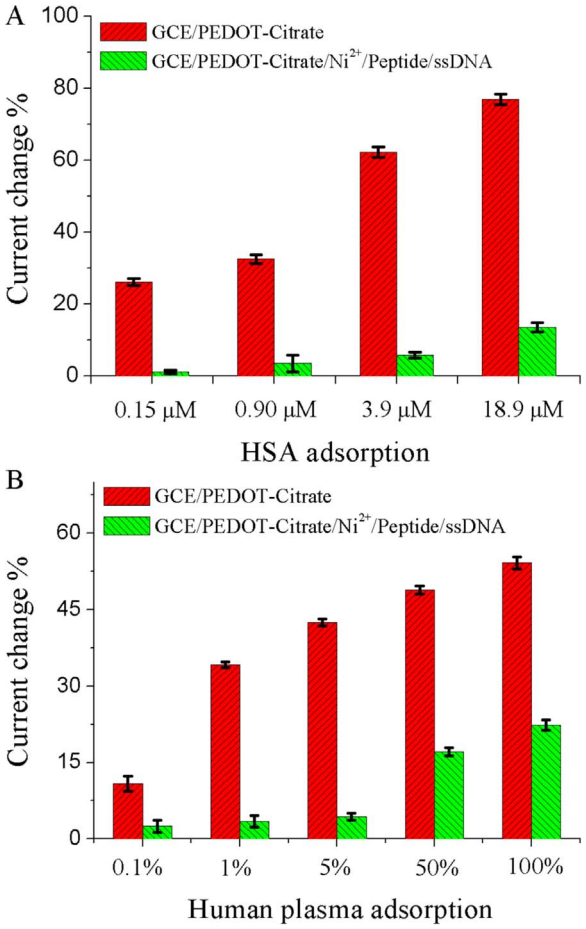

Fig. 5. Current changes of different electrodes after soaking in different solutions of HSA (A) and human plasma (B). Human plasma was diluted (v/v) with 10 mM pH 7.4 PBS containing 200 mM NaCl.

biosensor exhibited significantly smaller current change, whether after soaking in HSA or human plasma, indicating excellent antifouling ability of the sensing interface containing peptides (Chen et al., 2009; Leng et al., 2015).

Selectivity is an important criterion to evaluate a successful biosensor in target detection. In order to test the selectivity of the prepared biosensor for target DNA detection, several possible interferents including bovine serum albumin (BSA), one-base mismatch (M_1) sequences, three-base mismatch (M_2) sequences and complete mismatch (M_3) sequences were investigated. As shown in Fig. S4, the fabricated biosensor showed excellent selectivity toward its target DNA, and they showed negligible responses towards mismatched DNA or protein even at artificially high concentrations.

For the inter- and intra-sensor reproducibility tests, five sensors independently prepared were used to detect target DNA with the concentration of 10 nM, and the relative standard deviation (RSD) was 6.62%; the same biosensor was used to detect the same target DNA repetitively for five times, and the RSD was 1.75%. These results suggested an encouraging reproducibility of the prepared low fouling DNA biosensors.

3.6. Clinical application of the DNA sensor

To evaluate the practical application of the developed DNA biosensor, target DNA of various concentrations in 5% human plasma samples were measured. Before measurements, various concentrations of target DNA were doped into 5% human plasma samples. The assay results were summarized in Table S1 (see Supporting information), and the recovery was ranging from 97.80% to 103.88%, with RSD between 1.61% and 4.30%, evidencing ability of practical application of the developed gene biosensor in real samples.

4. Conclusion

In summary, a novel electrochemical gene biosensor based on low fouling peptide for the determination of breast cancer marker BRCA1 was successfully fabricated. Peptides terminated with carboxyl groups can be effectively anchored to citrate doped PEDOT via the coordination of nickel cations. In addition to their antifouling function, the anchored peptides also served as active substrate for DNA probe immobilization. In virtue of the excellent biocompatibility and remarkable antifouling ability of the peptide, the biosensor achieved high sensitivity and favorable selectivity, and was also efficient enough to detect BRCA1 in real complex samples, indicating feasible potential for practical application. This strategy for biosensor fabrication opened a promising avenue to construct other sensing systems capable of assaying in complex media.

Acknowledgments

This research was supported by the National Natural Science Foundation of China (21275087, 21422504, 21675093), the Natural Science Foundation of Shandong Province of China (JQ201406), the Taishan Scholar Program of Shandong Province of China (ts20110829), and the Domestic Visiting Scholar Program of

Shandong Province of China for Young Backbone Teachers of Colleges and Universities.

Appendix A. Supporting information

Supplementary data associated with this article can be found in the online version at doi:10.1016/j.bios.2016.10.088.

References

Bolduc, O.R., Pelletier, J.N., Masson, J.F.O., 2010. Anal. Chem. 82 (9), 3699–3706.
Chang, Y., Shih, Y.J., Lai, C.J., Kung, H.H., Jiang, S., 2013. Adv. Funct. Mater. 23 (9), 1100–1110.
Chen, S., Cao, Z., Jiang, S., 2009. Biomaterials 30 (29), 5892–5896.
Cui, M., Song, Z., Wu, Y., Guo, B., Fan, X., Luo, X., 2016. Biosens. Bioelectron. 79, 736–741.
Dollimore, L., Gillard, R., 1973. J. Chem. Soc. Dalton Trans. 9, 933–939.
Imani, R., Pazoki, M., Tiwari, A., Boschloo, G., Turner, A.P., Kralj-Iglic, V., Iglic, A., 2015. Nanoscale 7 (23), 10438–10448.
Kuhl, C.K., Schmutzler, R.K., Leutner, C.C., Kempe, A., Wardelmann, E., Hocke, A., Maringa, M., Pfeifer, U., Krebs, D., Schild, H.H., 2000. Radiology 215 (1), 267–279.
Ladd, J., Taylor, A.D., Piliarik, M., Homola, J., Jiang, S., 2009. Anal. Bioanal. Chem. 393 (4), 1157–1163.
Leng, C., Hung, H.C., Sun, S., Wang, D., Li, Y., Jiang, S., Chen, Z., 2015. ACS Appl. Mater. Interfaces 7 (30), 16881–16888.
Li, Y., Wang, Z., Ou, L.M., Yu, H.Z., 2007. Anal. Chem. 79 (2), 426–433.
Lowe, S., O'Brien-Simpson, N.M., Connal, L.A., 2015. Polym. Chem. 6 (2), 198–212.
Ludwig, T., Chapman, D.L., Papaioannou, V.E., Efstratiadis, A., 1997. Genes Dev. 11 (10), 1226–1241.
Luo, X., Davis, J.J., 2013. Chem. Soc. Rev. 42 (13), 5944–5962.
Luo, X., Xu, M., Freeman, C., James, T., Davis, J.J., 2013. Anal. Chem. 85 (8), 4129–4134.
Luo, X., Xu, Q., James, T., Davis, J.J., 2014. Anal. Chem. 86 (11), 5553–5558.
Nowinski, A.K., Sun, F., White, A.D., Keefe, A.J., Jiang, S., 2012. J. Am. Chem. Soc. 134 (13), 6000–6005.
Skolnick, M.H., 1994. Science 266 (5172), 66–71.
Stockhausen, V., Trippé-Allard, G., Van Quynh, N., Ghilane, J., Lacroix, J.C., 2015. J. Phys. Chem. C 119 (33), 19218–19227.
Sundaram, H.S., Han, X., Nowinski, A.K., Brault, N.D., Li, Y., Ella-Menye, J.R., Amoaka, K.A., Cook, K.E., Marek, P., Senecal, K., Jiang, S., 2014. Adv. Mater. Interfaces 1 (6), 1400071–1400078.
Vaisocherová, H., Brynda, E., Homola, J., 2015. Anal. Bioanal. Chem. 407 (14), 3927–3953.
Wang, D., Zheng, Y., Chai, Y., Yuan, Y., Yuan, R., 2015a. Chem. Commun. 51 (52), 10521–10523.
Wang, W., Fan, X., Xu, S., Davis, J.J., Luo, X., 2015b. Biosens. Bioelectron. 71, 51–56.
Weng, S., Li, X., Niu, M., Ge, B., Yu, H.Z., 2016. Anal. Chem. 88 (13), 6889–6896.
Wu, L., Qu, X., 2015. Chem. Soc. Rev. 44 (10), 2963–2997.
Wu, Z.K., Zhou, D.M., Wu, Z., Chu, X., Yu, R.Q., Jiang, J.H., 2015. Chem. Commun. 51 (14), 2954–2956.
Xu, C., Hu, X., Wang, J., Zhang, Y.-M., Liu, X.-J., Xie, B.-B., Yao, C., Li, Y., Li, X.-S., 2015. ACS Appl. Mater. Interfaces 7 (31), 17337–17345.
Yao, H., Zhang, Y., Xiao, F., Xia, Z., Rao, J., 2007. Angew. Chem. Int. Ed. 46 (23), 4346–4349.
Ye, H., Wang, L., Huang, R., Su, R., Liu, B., Qi, W., He, Z., 2015. ACS Appl. Mater. Interfaces 7 (40), 22448–22457.
Yoshimoto, K., Hirase, T., Madsen, J., Armes, S.P., Nagasaki, Y., 2009. Macromol. Rapid Commun. 30 (24), 2136–2140.